

## Phase-Transition-Induced Defect Formation in III-V Semiconductors

J. Crain, G. J. Ackland, R. O. Piltz, and P. D. Hatton

Department of Physics, The University of Edinburgh, Mayfield Road, Edinburgh, EH9 3JZ, Scotland  
(Received 13 July 1992)

We present experimental and theoretical evidence for the creation of inversion domain boundaries (IDBs) at structural phase transitions in III-V semiconductors. A novel use of anomalous high-pressure powder x-ray diffraction with an image plate area detector allows for the study of weak difference scattering, the absence of which is attributed to IDBs. As a test of this, *ab initio* total energy pseudopotential calculations, including both ionic relaxation and boundary layer expansion, have been performed on a particular type of possible defect—a (110) IDB in InSb.

PACS numbers: 61.72.Nn, 64.70.Kb, 71.45.Nt

The high-pressure properties of III-V semiconductors have been the subject of a vast amount of attention over the past thirty years. Like group-IV elements, III-V compounds exhibit a pressure-induced metallization transition from the zinc-blende (ZB) structure. We have recently investigated the high-pressure structures using a new technique—the image plate. Evidence from these and other studies suggests a dislocation-type mechanism for the transition, leaving as its signature a high concentration of planar defects.

The image plate is an x-ray detection system, applied to powder diffraction studies at high pressure [1]. It comprises a phosphor area detector which intercepts the entire Debye-Scherrer cone of diffracted radiation and stores the image as semistable color centers. Azimuthal integration around the diffraction rings gives patterns [2] of unprecedented sensitivity and signal-to-noise ratio. Details of the experimental arrangement have been reported elsewhere [1], but we note in particular that to enhance the difference between In and Sb scattering factors, a synchrotron x-ray wavelength near to the In absorption edge was required (0.44 Å).

Theoretical understanding of the structural stability of III-V compounds and the related group-IV elements in their ambient and high-pressure phases proceeded rapidly after the development of first-principles methods [3] and combinations of *ab initio* and empirical formulations [4]. The result of these efforts is a global picture of structure adoption in the  $A^N B^{8-N}$  family of semiconductors based on total energy comparison between plausible structures in which ionicity and bond length determine the preferred atomic arrangement in the unit cell. Within this framework, the more covalently bonded compounds generally exhibit a ZB to  $\beta$ -Sn transition under pressure, whereas a ZB to NaCl structural transition is expected for more ionic compounds.

InSb represents a known exception to this simple empirical rule [5]: It adopts an orthorhombically distorted crystal structure with a body centered orthorhombic (BCO) unit cell at high pressure. The first definitive structural determination of this phase including the site ordering of the nearly isoelectronic In/Sb was possible

due to the high sensitivity of the image plate [6,7]. We have also observed an intermediate transition in InSb from ZB to  $\beta$ -Sn (the diffraction pattern of which is shown in Fig. 1) above 20 kbar. Over time or under slight pressure increase (less than 2 kbar), the  $\beta$ -Sn phase was observed to transform to the BCO structure. In addition to the transitions noted above, further pressurization results in the formation of yet another orthorhombic unit cell of even greater complexity [7]. The diffraction pattern of the  $\beta$ -Sn phase differs in character from that collected in the BCO phase in that the diffraction peaks

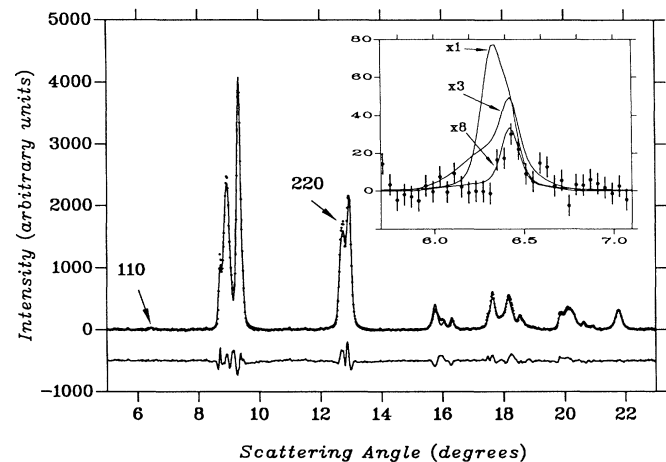


FIG. 1. Two-phase ( $\beta$ -Sn, 80%; BCO, 20%) Reitveld refinement of InSb obtained at 25 kbar. The refinement of the BCO component was performed assuming the  $Imm2$  space group. Observed intensities less a smoothly varying background are shown by dots. A displaced difference plot is also shown. The positions of the 110 and 220 reflections for the  $\beta$ -Sn phase are indicated. The inset shows an expanded section around the 110 difference peak positions of the  $\beta$ -Sn and BCO phases. The three calculated lines correspond to IDB models for the  $\beta$ -Sn phase which preferentially broaden the 110 difference peak relative to the 220 in-phase peak by factors of  $\times 1$ ,  $\times 3$ , and  $\times 8$ . The  $\times 8$  line is indistinguishable from the calculated profile of the 110 reflection from the BCO phase.

are significantly broader and the strongest “difference” peak (due to In/Sb out-of-phase scattering), which was essential in the BCO structure solution [7], is not observed. As the presence of such a peak requires In/Sb ordering, the traditional interpretation of such an absence is that this phase is site disordered. This explanation, however, is not consistent with the observed simple transition to the ordered BCO structure which would require a large degree of diffusion.

Recovered (depressurized) samples of InSb and GaSb were also investigated in order to determine the nature and completeness of the retransformation to the ZB phase. It was found that the ZB lattice is recovered in both cases, albeit with broadened peaks; the difference peak is not observed although it may be difficult to detect due to peak overlap in the ZB phase. In contrast to the  $\beta$ -Sn phase, the recovered samples show significant increasing peak width with increasing scattering angle ( $2\theta$ ).

Peak broadening in powder diffraction is indicative of extended crystal imperfections, such as small crystallite size, inhomogeneous strains, or planar defects separating the crystallites into small coherent domains. The observed peak broadening and lack of difference scattering in both the  $\beta$ -Sn and recovered ZB forms can be explained by the presence of a high concentration of phase-transition-induced planar defects. The broad in-phase peaks of both forms are consistent with a network of twins occurring on average every 200–400 Å. The  $2\theta$  dependence of the peak broadening for the recovered ZB phase is indicative of considerable internal crystal strain induced by the 20% volume change at the  $\beta$ -Sn–Zb transition. In contrast, the  $\beta$ -Sn phase is comparatively strain-free probably due to high dislocation mobility in the metallic phase. Normally, a domain boundary disrupts the arrangement of scattering sites; however, for an IDB the arrangement of sites is preserved with the atomic species interchanged (Fig. 2). Therefore the presence of IDBs will not affect those reflections which are due to the constructive interference from all scattering sites, i.e., the in-phase reflections. However, the presence of IDBs will affect the difference reflections causing these powder lines to broaden relative to the in-phase ones [8]. Analysis of powder linewidths of the  $\beta$ -Sn phase (Fig. 1) indicates that the 110 difference peak is at least 8 times broader than the 220 in-phase peak, a degree of broadness which renders the difference peak indistinguishable from a smoothly varying background. Of possible extended crystal imperfections (including an orthorhombic distortion of the  $\beta$ -Sn phase), only the presence of IDBs can cause such a preferential broadening of the 110 peak. The lower limit placed on the width of the 110 difference peak suggests an upper limit of 50 Å on the mean IDB separation.

Even though the types and orientations of the planar defects cannot be determined uniquely in our experiment,

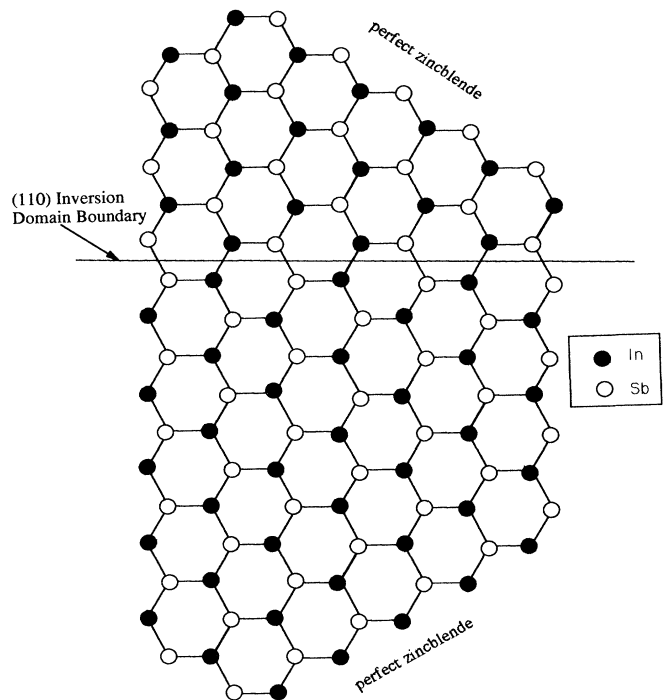


FIG. 2. A projection of the (110) stoichiometric inversion domain boundary in the ZB structure of InSb.

the (110) IDB has been observed in the ZB phase of GaAs [9]. We therefore adopt the (110) IDB as our model defect in the ZB phase of InSb and attempt to ascertain its formation energy. A recent linear muffin-tin orbital calculation of the equivalent boundary in GaAs indicated that it was of low energy [10].

In order to obtain a quantitative estimate of the energy cost in forming such a boundary, we have performed *ab initio* total energy pseudopotential calculations on a twelve-atom InSb supercell representing the (110) IDB (a projection of which is shown in Fig. 2). This boundary can be represented by uncharged supercells. The computationally intensive nature of these calculations compounded by the essential inclusion of ionic relaxation has rendered them intractable until recently. The calculations were performed exclusively on the *i*860-based Parallel Supercomputer at the University of Edinburgh running the CETEP code [11], which employs a density functional framework and a local density approximation to exchange and correlation [12]. Pseudopotentials of the Kleinman-Bylander type [13] were generated using the Kerker method [14] with a relativistic correction. Details and extensions of these calculations will be presented in a forthcoming article [15]. Within this formalism, the total energy of the system is given by a functional,  $E$ , of the electronic wave function and ionic positions  $\{\psi_i\}$  and  $\{R_i\}$ , respectively, such that

$$E[\{\psi_i\};\{R_I\}] = \sum_{i=1}^{(\text{occ state})} \int [\psi_i^*(r)\nabla^2\psi_i(r)]dr + \int V_{ps}(r)\rho(r)dr + \frac{1}{2} \int \int \frac{\rho(r)\rho(r')}{|r-r'|} dr dr' + \frac{1}{2} \sum_{I \neq I'} \frac{Z_I Z_{I'}}{|R_I - R_{I'}|} + E_{xc}[\rho(r)].$$

The energy functional is minimized with respect to  $\{\psi_i\}$  (expanded in a plane wave basis set),  $\{R_I\}$ , and cell dimensions which act as variational parameters in the minimization process and  $\{\psi_i\}$  correspond to the Kohn-Sham eigenstates at the minimum of  $E[\{\psi_i\};\{R_I\}]$ . The terms in the functional represent the kinetic, electron-core, Hartree, Madelung, and exchange-correlation contributions, respectively.  $V_{ps}$  and  $\rho(r)$  are, respectively, the pseudopotential and charge density. A conjugate gradients minimization routine is used to relax the electronic configuration to its ground state for fixed ionic positions. Ionic relaxation proceeds by a steepest-descent algorithm.

The supercell dimensions ( $a=6.273 \text{ \AA}$ ,  $b=4.435 \text{ \AA}$ , and  $c=13.307 \text{ \AA}$ ) were obtained by minimizing total energy with respect to cell volume for the perfect lattice and are approximately 3.0% smaller than the room-temperature experimental lattice constant of InSb. In inset (a) of Fig. 3, the IDB supercell is shown, illustrating two pairs of "wrong" bonds. The  $a$  and  $b$  must be commensurate with the perfect structure and are therefore fixed. The  $c$  dimension is free to expand. For the case of the perfect supercell [shown in inset (b) of Fig. 3], four special  $k$  points were sampled with a 400 eV cutoff for plane waves. Calculations proceeded until energy convergence was better than  $10^{-4}$  eV. The calculation of total energy

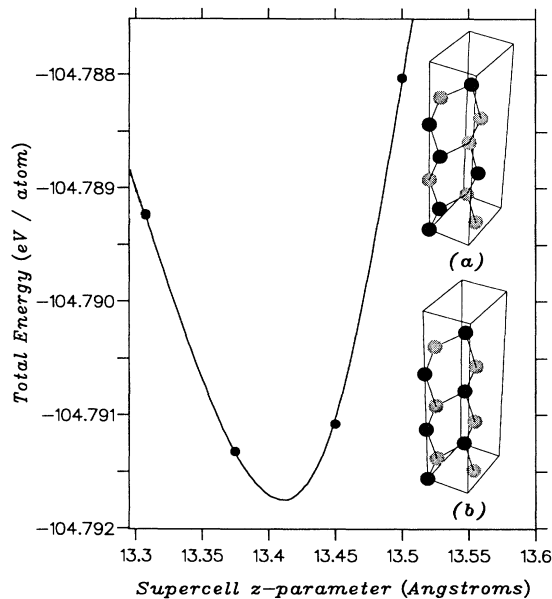


FIG. 3. Total energy of an InSb supercell representing a (110) IDB as a function of  $c$ -axis lattice constant ( $z$  parameter). Inset (a) shows the geometry of the supercell used in the calculations to model the InSb (110) IDB. The perfect supercell is shown in inset (b) for comparison.

for the IDB supercell was carried out using identical zone sampling, energy cutoff, and  $a$  and  $b$  cell dimensions but allowing for relaxation parallel to the  $c$  axis as demanded by symmetry. In addition, the positions  $\{R_I\}$  of all twelve atoms of the supercell were allowed to relax under the influence of the Hellmann-Feynman forces. An expansion of the IDB supercell  $c$ -lattice parameter of 0.05  $\text{\AA}$ /boundary was obtained from the calculation relative to the perfect structure as shown in Fig. 3. In addition, a contraction (expansion) of approximately 1% was observed for the In-In (Sb-Sb) bond lengths. It is found that the energy difference between this fully relaxed structure and the perfect supercell implies a value for the IDB energy of  $310 \text{ mJm}^{-2}$  which gives an energy of  $0.285 \text{ eV/(wrong bond)}$ . In the unrelaxed structure a value of  $0.35 \text{ eV/(wrong bond)}$  ( $380 \text{ mJm}^{-2}$ ) is obtained which is close to the value of  $0.38 \text{ eV/(wrong bond)}$  reported for the (110) IDB in unrelaxed GaAs [10] using a localized basis-set technique for which a Hellmann-Feynman force determination cannot be reliably performed. We expect the IDB formation energies in InSb and GaAs to be roughly equal due to their similar size ratios and ionicities. We note that the IDB formation energy for the relaxed geometry is roughly 25% lower than in the unrelaxed case, implying that ionic positional relaxation and to a lesser extent unit cell relaxation are required for accurate determination of formation energies.

Using the results of these calculations we can compare the energies of the IDB microstructure and the site-disordered structure. Site disorder up to the percolation threshold (i.e., that sufficient to destroy long-range order) requires an order of magnitude more wrong bonds than the  $50 \text{ \AA}$  IDB microstructure. Assuming that the wrong bond energy is similar in both cases, site disorder requires an energy of about  $0.45 \text{ eV/atom}$ . The phase transition occurs with a 20% volume collapse supplying about  $0.08 \text{ eV/atom}$  ( $P\Delta V$ ). This provides insufficient energy to cause site disorder throughout the crystal. Thus site disorder appears to be improbable not only in view of the rapid transition to an ordered BCO phase but also on energetic grounds. However, under pressure, formation of localized regions of the  $\beta$ -Sn phase may concentrate sufficiently large stresses resulting in nucleation and/or motion of partial dislocations which create IDBs as they glide. The energy required to form the  $50 \text{ \AA}$  IDB microstructure (about one boundary every ten layers) is, on average,  $0.05 \text{ eV/atom}$  and could, therefore, be supplied by the phase transition.

We have outlined a novel use of anomalous high-pressure powder x-ray diffraction using an image plate area detector system which allows for routine determination of the presence or absence of weak features in diffraction patterns such as InSb difference reflections.

In the present case such a capability has provided evidence for the phase-transition-induced formation of several types of planar defects in III-V semiconductors which persist in the recovered ambient pressure cubic form. These results have motivated a preliminary *ab initio* study of IDB energetics in InSb which suggests low formation energies for 50 Å inversion domains relative to site disorder. It is the combination of the experimental evidence and the results of the total energy calculations that provides a persuasive argument against site disorder in InSb. Furthermore, an ordered structure with a high concentration of IDBs appears to be the only model which is both energetically plausible and consistent with the diffraction results.

This work was supported by the SERC. J.C. acknowledges a departmental scholarship from the University of Edinburgh. G.J.A. acknowledges support from the UK Grand Challenge Project and BP via the Royal Society of Edinburgh. The authors also acknowledge R. J. Nelmes and M. I. McMahon for the experimental aspects of this work, M. C. Payne, I. Štich, V. Milman, and V. Heine for valuable discussions as well as J. S. Lin for the generation of pseudopotentials.

---

[1] R. J. Nelmes, P. D. Hatton, M. I. McMahon, R. O. Piltz, J. Crain, R. J. Cernik, and G. Bushnell-Wye, *Rev. Sci.*

- Instrum.* **63**, 1039 (1992).
- [2] R. O. Piltz, M. I. McMahon, J. Crain, P. D. Hatton, R. J. Nelmes, R. J. Cernik, and G. Bushnell-Wye, *Rev. Sci. Instrum.* **63**, 700 (1992).
- [3] M. T. Yin and M. L. Cohen, *Phys. Rev. B* **26**, 5668 (1982).
- [4] J. R. Chelikowsky, *Phys. Rev. B* **35**, 1174 (1987).
- [5] M. D. Banus and M. C. Lavine, *J. Appl. Phys.* **40**, 409 (1968).
- [6] R. J. Nelmes, P. D. Hatton, M. I. McMahon, R. O. Piltz, and J. Crain, in *Proceedings of the Thirteenth AIRAPT International Conference on High Pressure Science and Technology*, edited by A. K. Singh (Oxford & IBH Publishing Co., New Delhi, 1992), p. 753.
- [7] R. J. Nelmes, M. I. McMahon, P. D. Hatton, J. Crain, and R. O. Piltz, *Phys. Rev. B* **47**, 35 (1993).
- [8] B. E. Warren, *X-Ray Diffraction* (Dover, London, 1991).
- [9] D. R. Rasmussen, S. MacKernan, and C. B. Carter, *Philos. Mag. A* **63**, 1299 (1991).
- [10] W. R. Lambrecht, C. Amador, and B. Segall, *Phys. Rev. Lett.* **69**, 1363 (1992).
- [11] I. Štich, M. C. Payne, R. D. King-Smith, J. S. Lin, and L. J. Clarke, *Phys. Rev. Lett.* **68**, 1351 (1992).
- [12] J. P. Perdew and A. Zunger, *Phys. Rev. B* **23**, 5048 (1981).
- [13] L. Kleinman and D. M. Bylander, *Phys. Rev. Lett.* **48**, 1425 (1982).
- [14] G. P. Kerker, *J. Phys. C* **13**, L189 (1990).
- [15] G. J. Ackland, J. Crain, P. D. Hatton, I. Štich, M. C. Payne, J. S. Lin, and L. Clark (unpublished).